



TITLE:

Bifurcation diagrams in Kolmogorov's  
problem of viscous incompressible fluid on  
2-D flat tori(Instability of Flows and Vortex  
Structure of Turbulent Flows)

AUTHOR(S):

OKAMOTO, H.; SHOJI, M.

---

CITATION:

OKAMOTO, H. ...[et al]. Bifurcation diagrams in Kolmogorov's problem of viscous incompressible fluid on 2-D flat tori(Instability of Flows and Vortex Structure of Turbulent Flows). 数理解析研究所講究録 1991, 767: 29-51

ISSUE DATE:

1991-09

URL:

<http://hdl.handle.net/2433/82312>

RIGHT:

## Bifurcation diagrams in Kolmogorov's problem of viscous incompressible fluid on 2-D flat tori.

H. OKAMOTO<sup>1</sup> AND M. SHŌJI<sup>2</sup>,

**Abstract.** We consider Kolmogorov's problem of a viscous incompressible fluid motion on two dimensional tori. In a previous paper [13], we computed stationary flows numerically. One of the new discovery is the existence of turning points in the primary branch from the basic flow. In the present paper we continue to study the structure of bifurcation by a numerical method. In [13] we computed only the branch of mode one. In the present paper we compute branches of mode two and three as well as that of mode one. We find that there are secondary bifurcations in the branches of mode two and three. Furthermore, Hopf bifurcation points are also found when the aspect ratio of the torus satisfies a certain condition.

### §1. Introduction.

Kolmogorov's problem mentioned above was suggested by him in 1959 ( see Obukhov [20] for history ). The problem is to solve the Navier-Stokes equations in two dimensional flat tori under a special driving force. More precisely, we solve the Navier-Stokes equations

$$(1.1) \quad \frac{\partial u}{\partial t} + u \frac{\partial u}{\partial x} + v \frac{\partial u}{\partial y} = \nu \Delta u - \frac{1}{\rho} \frac{\partial p}{\partial x} + \gamma \sin(\pi y/b),$$

$$(1.2) \quad \frac{\partial v}{\partial t} + u \frac{\partial v}{\partial x} + v \frac{\partial v}{\partial y} = \nu \Delta v - \frac{1}{\rho} \frac{\partial p}{\partial y},$$

$$(1.3) \quad \frac{\partial u}{\partial x} + \frac{\partial v}{\partial y} = 0,$$

where  $(u, v)$ ,  $p$ ,  $\rho$ ,  $\nu$  are velocity vector, pressure, mass density and the kinematic viscosity, respectively. The flow region is a rectangle  $[-a, a] \times [-b, b]$  and the periodic boundary condition is imposed in both directions. We try to understand how the stationary or time-periodic solutions depend on the aspect ratio  $\alpha \equiv b/a$  and the Reynolds number which is defined in §2. More complicated solutions such as quasiperiodic solutions or chaotic trajectories are out of scope of the present paper, although we discuss in the last section relations to other works dealing with time dependent solutions. We wish to see the global structure of the bifurcations. Here, ' global ' means that we consider the whole range of the Reynolds number. We will show that it may be possible to understand the global structure of the stationary Navier-Stokes flows on a 2-D flat torus driven by a special force proposed by Kolmogorov. Our motivation, like Kolmogorov's one, is a hope that we can investigate viscous fluid

<sup>1</sup>Research Institute for Mathematical Sciences, Kyoto University, Kyoto 606 Japan

<sup>2</sup>Dept. of Mathematics, Faculty of Science, University of Tokyo, Bunkyo-ku, Tokyo 113 Japan

motion most rigorously and most extensively by considering the simplest case. For instance, if  $\alpha$  is not too small, we find a family of stationary solutions which undergo no instability even when the Reynolds number tends to infinity. Such a rather simple structure of solutions seems to support our hope.

A nondimensional form is given in §2 and a certain symmetry of the equation is revealed. In §3 we review a mathematical theory of the linearized operator at the basic laminar flow. In §4 we consider solutions of mode one. Mode is, roughly speaking, the numbers of pairs of vortices in the rectangle. Solutions of mode two are discussed in §5. §6 deals with solutions of mode three.

**Acknowledgement.** The present work was partially supported by Ohbayashi Corporation. The figures were prepared by the package program GLSC, which was given to the authors by Dr. R. Kobayashi. We cordially thank him.

## §2. Nondimensionalization.

In this section we transform (1.1-3) into a nondimensional form. We introduce a stream function  $\psi$ . Thus the components of the velocity field are  $u = \psi_y$  and  $v = -\psi_x$ . Here and hereafter the subscripts mean differentiations. The equations (1.1-3) are equivalent to :

$$(2.1) \quad \frac{\partial}{\partial t} \Delta \psi - \nu \Delta^2 \psi - J(\psi, \Delta \psi) = \frac{\gamma \pi}{b} \cos(\pi y/b),$$

where  $J$  is a bilinear form defined by

$$J(u, v) = \frac{\partial u}{\partial x} \frac{\partial v}{\partial y} - \frac{\partial u}{\partial y} \frac{\partial v}{\partial x}.$$

Our nondimensional form is obtained by the following transformation of variables:

$$(x', y') = \left( \frac{\pi x}{b}, \frac{\pi y}{b} \right), \quad \psi'(x', y') = \frac{\nu \pi^3}{\gamma b^3} \psi(x, y), \quad t' = \frac{\gamma b}{\nu \pi} t$$

We then define the Reynolds number  $R$  by

$$R = \frac{\gamma b^3}{\nu^2 \pi^3}.$$

After dropping the primes, we have the following equation:

$$(2.2) \quad \frac{\partial}{\partial t} \Delta \psi - \frac{1}{R} \Delta^2 \psi - J(\psi, \Delta \psi) = \frac{1}{R} \cos y.$$

This equation should be satisfied in  $[-\pi/\alpha, \pi/\alpha] \times [-\pi, \pi]$ , where  $\alpha = b/a$ . We denote this domain by the symbol  $\mathbb{T}_\alpha$  and call it a two dimensional flat torus of aspect ratio  $\alpha$ .

We assume that  $\psi$  is periodic in  $x$  and  $y$ . This does not exclude any interesting phenomena. In fact, integrating in  $\mathbb{T}_\alpha$ , we see that the spatial mean of  $(u, v)$  on  $\mathbb{T}_\alpha$  is constant in time. If we consider only those initial velocities whose spatial means are zero, then the mean velocity vanishes for all the time. If this is the case, it is obvious that the stream function  $\psi$  is periodic in  $\mathbb{T}_\alpha$ . We first note that  $\psi(t, x, y) \equiv -\cos y$  satisfies all the requirements for any  $R > 0$ . We call this a basic solution. The velocity field of the basic solution is given by  $(u, v) = (\sin y, 0)$ , which represents a shear flow parallel to the  $x$ -axis. Defining  $\phi$  by  $\phi = \psi + \cos y$ , we write (2.2) as follows:

$$(2.3) \quad \frac{\partial}{\partial t} \Delta \phi - \frac{1}{R} \Delta^2 \phi + \sin y (\Delta + I) \frac{\partial \phi}{\partial x} - J(\phi, \Delta \phi) = 0,$$

where  $I$  is the identity operator.

We now prove that the equation (2.2) has a certain symmetry, which helps us to better understand the bifurcation structure. We define an operator  $U$  and  $V_\beta$  ( $0 \leq \beta < 2\pi$ ) by

$$Uf(x, y) = f(-x, -y), \quad V_\beta f(x, y) = f(x + \beta, y).$$

These operators define an action of the group  $O(2)$  on the functions on  $\mathbb{T}_\alpha$ . We remark that  $V_\beta$  corresponds to the rotation of angle  $\beta$  and  $U$  the reflection. If the left hand side of (2.3) is denoted by  $F(\phi)$ , then it holds that

$$F(U\phi) = UF(\phi), \quad F(V_\beta\phi) = V_\beta F(\phi)$$

for all  $\beta \in [0, 2\pi)$  and all functions  $\phi$  for which  $F(\phi)$  can be defined. This property is called  $O(2)$ -equivariance of the mapping  $F$  with respect to the group  $O(2)$ . Other than  $U$  and  $V_\beta$ , there is another operator about which  $F$  is equivariant. It is given by

$$Wf(x, y) = -f\left(\frac{\pi}{\alpha} + x, \pi - y\right).$$

We can easily prove that  $F(W\phi) = WF(\phi)$ . We now define

$$\begin{aligned} X &= \{\phi \in H^4(\mathbb{T}_\alpha)/\mathbb{R}; \quad U\phi = \phi, \quad W\phi = \phi\}, \\ Y &= \{\phi \in H^4(\mathbb{T}_\alpha)/\mathbb{R}; \quad U\phi = \phi\}, \end{aligned}$$

where  $H^4(\mathbb{T}_\alpha)$  is a Sobolev space: namely the set of all the functions which, together with their derivatives of order  $\leq 4$ , are square integrable. The symbol  $/\mathbb{R}$  implies that only those functions with zero spatial mean are collected. We note that (2.2) generates a nonlinear semigroup in  $H^4(\mathbb{T}_\alpha)/\mathbb{R}$  and that both  $X$  and  $Y$  are positively invariant with respect to this semigroup. In a computation of the Navier-Stokes flows on 2-D and 3-D tori, Kida et al. [15,16] used special symmetries in order to get a large degree of freedom of differential equations. Our symmetry has a similar nature. In general, larger symmetry implies smaller function space and simpler structure of the set of solutions. The computation in [13] was carried out in the smallest function space  $X$  and relatively simple structure was found. In the present paper we consider solutions in  $Y$ , by which we obtain a somewhat richer structure in the solutions.

### §3. Solutions near the basic one: a rigorous result.

We first recall a fact which is known as “ the principle of exchange of stability ”. In order to study bifurcations from the basic flow  $\phi \equiv 0$ , we must solve the following linearized eigenvalue problem:

$$(3.1) \quad \sigma \Delta \phi - \frac{1}{R} \Delta^2 \phi + \sin y (\Delta + I) \frac{\partial \phi}{\partial x} = 0.$$

where  $\sigma$  is the eigenvalue. If all possible  $\sigma$ 's have negative real parts, the basic flow is stable. Meshalkin and Sinai [18] proved the principle of exchange of stability. Namely they proved:

**PROPOSITION 3.1.** *If (3.1) has an eigenvalue with  $\operatorname{Re}[\sigma] \geq 0$ , then it must be a real number.*

This proposition shows that the eigenvalues can cross the imaginary axis only at the origin and that only stationary solutions can bifurcate from the basic flow. We remark that eigenfunctions in Proposition 3.1 are sought in  $H^4(\mathbb{T}_\alpha)$ , not in our smaller space  $X$  or  $Y$ . Therefore the principle of exchange of stability holds not only in our restricted problem in  $X$  or  $Y$  but also in the situation with full generality. We should like to emphasize that the principle is proved on the basic flows. Therefore, bifurcation of time periodic solutions is not excluded along branches of solutions other than basic ones.

In view of the proposition above, we first consider stationary solutions to (2.2) in  $Y$ . Thus, we seek solutions to the following equations in  $Y$ :

$$(3.2) \quad \Delta^2 \psi + RJ(\psi, \Delta \psi) + \cos y = 0.$$

Solutions of mode one ( the meaning of mode will be defined later in this section ) in  $X$  is computed in [13]. We compute in a larger space  $Y$  the solutions of mode two and three as well as those of mode one.

We first characterize  $X$  and  $Y$  concretely. Suppose  $\psi \in H^4(\mathbb{T}_\alpha)/\mathbb{R}$  is expanded in the Fourier series as

$$\psi = \sum a_{m,n} e^{im\alpha x + iny},$$

where the summation is taken over all the pairs of integers but  $(m, n) = (0, 0)$ . Since  $\psi$  is real-valued, it holds that  $\overline{a_{m,n}} = a_{-m, -n}$ . If  $\psi$  satisfies  $U\psi = \psi$ , we have  $a_{m,n} = a_{-m, -n}$ . By this consideration, the function space  $Y$  has the following orthogonal decomposition:  $Y = Y_0 \oplus Y_1 \oplus Y_2 \oplus \cdots$ , where

$$Y_0 = \left\{ \sum_{n=1}^{+\infty} a_n \cos ny \mid a_n \in \mathbb{R}, \sum_{n=1}^{+\infty} (1+n^8) a_n^2 < +\infty \right\},$$

$$Y_m = \left\{ \sum_{n=-\infty}^{+\infty} a_n \cos(m\alpha x + ny) \mid a_n \in \mathbb{R}, \sum_{n=-\infty}^{+\infty} (1+n^8) a_n^2 < +\infty \right\} \quad (m \geq 1).$$

If  $\psi$  satisfies  $W\psi = \psi$ , we obtain  $a_{m,n} = (-1)^{m+n+1}a_{m,-n}$ . Consequently we have  $X = X_0 \oplus X_1 \oplus X_2 \oplus \dots$ , where

$$X_0 = \left\{ \sum_{n=1}^{+\infty} a_{2n-1} \cos(2n-1)y \mid a_{2n-1} \in \mathbb{R}, \sum_{n=1}^{+\infty} (1+n^8)a_{2n-1}^2 < +\infty \right\},$$

$$X_m = \left\{ \sum_{n=-\infty}^{+\infty} a_n \cos(m\alpha x + ny) \in Y_m \mid a_n \in \mathbb{R}, a_n = (-1)^{m+n+1}a_{-n} \right\} \quad (m \geq 1).$$

We consider the linearized operator at the basic solution, i.e.

$$(3.3) \quad L = L_{R,\alpha}\phi \equiv \Delta^2\phi - R \sin y (\Delta + I) \frac{\partial\phi}{\partial x}.$$

We denote by  $N(L; Z)$  the nullspace of  $L$  in  $Z$ , i.e.,

$$N(L; Z) = \{ u \in Z; \quad Lu = 0 \}.$$

The following lemma, which was proved by Iudovich [11], is the starting point of the mathematical analysis:

LEMMA 3.1. *There exists a continuous function  $R = R^*(\alpha)$  ( $0 < \alpha < 1$ ) such that :*

- i)  $R^*$  is a strictly monotone increasing function;
- ii)  $R^*(\alpha) \rightarrow +\infty$  as  $\alpha \rightarrow 1$ ;
- iii)  $R^*(\alpha) \rightarrow \sqrt{2}$  as  $\alpha \rightarrow 0$ ;

and that  $N(L_{R,\alpha}; Y_1)$  is nontrivial if and only if  $(R, \alpha) = (R^*(\alpha), \alpha)$ . If  $(R, \alpha)$  satisfies this, then  $N(L_{R,\alpha}; Y_1)$  is of one dimension.

We choose a function  $\phi_1 \not\equiv 0$  such that it spans  $N(L_{R^*(\alpha),\alpha}; Y_1)$ . By Lemma 3.1,  $\phi_1$  is determined uniquely modulo a multiplicative constant for each  $\alpha \in (0, 1)$ . For each positive integer  $m$ , we define  $\Gamma_m$  as the curve:  $R = R^*(m\alpha)$  ( $0 < \alpha < 1/m$ ). These curves are called neutral curves or bifurcation curves. We also define a function  $\phi_m(x, y) = \phi_1(mx, y)$ .

The following lemma is proved in [13].

LEMMA 3.2.  $N(L_{R,\alpha}; Y)$  is nontrivial if and only if  $(R, \alpha) \in \Gamma_m$  for some positive integer  $m$ . If  $(R, \alpha) \in \Gamma_m$ , then  $\phi_m$  spans  $N(L_{R,\alpha}; Y)$ . If  $m$  is odd, then  $N(L_{R,\alpha}; X_m) = N(L_{R,\alpha}; Y_m)$ . If  $m$  is even, then  $N(L_{R,\alpha}; X_m) = \{0\}$ .

COROLLARY.

$$N(L_{R,\alpha}; Y) = \bigoplus_{m=1}^{\infty} N(L_{R,\alpha}; Y_m)$$

where at most one member of the right hand side is nontrivial. In particular,  $N(L; Y)$  is at most of one dimension.

The assertion iii) of Lemma 3.1 seems to be proved by many people independently later ([8,10]). The picture of the curves  $\Gamma_m$  are given in Fig.1. We remark that the set of bifurcation points in  $X$  is composed of  $\Gamma_{2k-1}$  with  $k = 1, 2, \dots$  (Lemma 3.2). Since there is no bifurcation point in  $\alpha \geq 1$ , it is natural to imagine that the dynamics is simple when  $\alpha \geq 1$ . In fact Iudovich proved the following remarkable theorem:

**THEOREM 3.1** ( IUDOVICH [11] ). For any  $1 \leq \alpha < +\infty$ ,  $0 < R < \infty$  and any initial value  $\phi(0, x, y) \in H^4(\mathbb{T}_\alpha)/\mathbb{R}$ , the solution to (2.3) decays exponentially toward the zero solution as  $t \rightarrow +\infty$ . Namely the basic solution is globally stable for any Reynolds number if  $\alpha \geq 1$ .

**Remark.** Marchioro [17] rediscovered this theorem recently, although his result is slightly more general than Iudovich's. For the proof of Theorem 3.1, see [11]. See also [17].

In [11], Iudovich proved that every point of  $\Gamma_m$  is a bifurcation point. Namely every neighborhood of a point  $\in \Gamma_m$  contains a solution other than the basic one. He also proved, by computing a topological degree, that for all  $(R, \alpha)$  satisfying  $R > R^*(\alpha)$ , there exists at least one solution to (3.2) other than  $\psi = -\cos y$ . Although he did not mention, it is easy to prove that, for a fixed  $\alpha \in (0, 1)$ , there is a curve of nontrivial solutions which emanates from  $(R^*, 0)$  and makes a pitchfork together with the  $R$ -axis in a neighborhood of the bifurcation point. By making use of the symmetry with respect to  $W$ , it is easy to see that the curves of nontrivial solutions from  $(R^*(k\alpha), 0)$  with odd  $k$  lie in  $X$ .

It is also easy to verify that if  $(R, \psi(x, y))$  solves (3.2) in  $\mathbb{T}_\alpha$ , then  $(R, \psi(mx, y))$  satisfies (3.2) in  $\mathbb{T}_{\alpha/m}$  for any positive integer  $m$ . Therefore the existence of a branch emanating from  $\Gamma_1$  implies the existence of that from  $\Gamma_m$  ( $m = 1, 2, \dots$ ). Those solutions on the branch from  $\Gamma_m$  are called solutions of mode  $m$ .

There are papers which consider the problem with different forcing. These include [2,5-8,12,21,23,24]. One characteristic of Kolmogorov's problem is that there is no bifurcation point of multiplicity  $\geq 2$ . Namely each  $\Gamma_m$  does not intersect other  $\Gamma_n$  ( $n \neq m$ ). If a different force is assumed, neutral curves of different modes do intersect ( e.g., [2,23] ).

#### §4. Stationary solutions of mode one.

As is mentioned above, the only rigorous results is that there is at least one solution if  $R > R^*(\alpha)$ . Some interesting questions seem to be open. For instance, existence of secondary or tertiary bifurcations, existence of turning points, stability of them and the asymptotic behavior of stationary solutions as  $R \rightarrow \infty$  should be clarified. Also the existence of Hopf bifurcation is a big problem. They are prohibited to occur at the branch of basic solutions ( Proposition 3.1 ) but there is a possibility that time-periodic solutions can bifurcate from the branch of other stationary solutions guaranteed by Iudovich. Although the details are presented later in this paper, we here list some new facts:

- a) For some  $\alpha < 1$ , solutions different from the basic one can exist in the range  $R < R^*(\alpha)$ .
- b) Time periodic solutions bifurcate.
- c) Some stationary solutions with cat's eyes pattern recover stability.

According to usual scenario, the steady states are unstable for Reynolds numbers above a certain critical value and are replaced by other steady-states or periodic solutions. After bifurcating a few times, a chaotic regime appears and becomes dominant

in the phase space. Our numerical solutions did not display transition of this kind, at least when  $\alpha = 0.7$ . Below we present our numerical result, in which solutions are sought in  $Y$ .

We first describe our scheme of discretization. We consider the following finite Fourier series:

$$\psi = \sum_{m=-M}^M \sum_{n=-N}^N a(m, n) e^{im\alpha x + iny},$$

Here  $a(0, 0) = 0$ . Since  $\psi$  is sought in  $Y$ , the coefficients satisfy  $a(m, n) = a(-m, -n)$  and they are real numbers. Substituting this approximate representation into (3.2), we let the Fourier coefficients of the resulting equation be zero for  $|m| \leq M, |n| \leq N, (m, n) \neq (0, 0)$ . In this way we obtain  $(2m + 1)(2n + 1) - 1$  equations for the same number of unknowns. By the symmetry just mentioned, the degree of freedom reduces by a half. When we have a solution  $(R, \psi)$  at an ordinary point of a path, we compute  $(R + \delta R, \psi + \delta \psi)$  by the Newton method using  $(R, \psi)$  as an initial guess. When we come to a turning point or a bifurcation point, we follow Keller's algorithm ([14]). For most computations with  $\alpha > 0.3$ , it is sufficient to choose  $M = N = 16$ . In this case, the degree of freedom is 544. When  $\alpha$  is small we have to choose a large  $M$ . For  $\alpha = 0.2$ , we choose  $M = 28$  and  $N = 16$ . For  $\alpha = 0.1$ , we choose  $M = 32$  and  $N = 12$ .

In the present paper we consider  $R$  as a bifurcation parameter and  $\alpha$  as a supplementary, splitting parameter. We first consider the case of  $\alpha = 0.7$ . In this case, the basic flow loses stability at  $R = R^*(0.7) \approx 3.011193 \dots$  and another steady state bifurcates. The bifurcation is *supercritical*. What is interesting is that we could not find any secondary bifurcation from this branch in  $Y$  nor we found any turning point. Accordingly, we have a bifurcation diagram like Fig.2, where the  $R$ -axis consists of the basic solutions. The bifurcating numerical solutions have a definite limit as  $R \rightarrow +\infty$ . Fig.3 shows the stream lines of six solutions on the bifurcating branch. Note that all the stream lines of the basic flows are parallel to the  $x$ -axis. In these figures, we can observe a pair of vortices: one with positive vorticity and another negative. Solutions on another side of the pitchfork are obtained by shifting these solutions to the  $x$ -direction by half a wave length. Steady flows of this nature are obtained in Bondarenko et al. [4] and Franceschini et al. [5], although their problems differ from ours. [4] deals with a laboratory experiments of thin films of an electrolyte. [5] deals with a numerical computation of the two dimensional Navier-Stokes equations in flat torus. But they assume a driving force different from ours. As we pursue the branch, we computed numerically the eigenvalues of the matrix which results from the linearization at the bifurcating solution. As far as we can compute, every eigenvalue lies in the left half-plane. We verified this for a Reynolds number up to 10,000.0. By this we conclude that there is no secondary bifurcation when  $\alpha = 0.7$ .

As we trace the branch we notice a substantial change in the topology of the stream lines ( Fig.3 ). Indeed, for  $R^*(0.7) < R < 4.61 \dots$ , the vortex on the center is oblate. The boundary of the vortex is composed of two homoclinic trajectories. At



$R = 4.61 \dots$ , the boundary of the vortex is composed of four heteroclinic trajectories. For  $4.61 \dots < R$  the vortices are prolate. The variation of vortices like this is reported in [3] and their scenario fits ours very well. However, in the paper they also claimed that each vortex is broken into a pair of smaller vortices for sufficiently large Reynolds numbers. This final stage is not observed in our computation. We believe ours is more accurate than theirs, since they drew figures based on a certain rough approximation. Their approximate solution is obtained by truncating the Navier-Stokes equations but the degree of freedom of the resulting ordinary differential equations is only *three*. As  $R \rightarrow \infty$  their approximate solution approaches zero. On the other hand, our computation shows that the bifurcating solution approaches a certain limit which is non-zero. Consequently we suspect that their approximate solution is valid up to only a moderately large Reynolds number.

We computed solutions of mode 1 with other values of  $\alpha$ . We found that for  $0 < \alpha < 0.966 \dots$ , *the solutions of mode 1 consists only of a pitchfork*. Fig. 4 shows the bifurcation diagrams of mode one when  $\alpha = 0.1$  and  $0.33$ , respectively. Recall that the Navier-Stokes equations are equivariant with respect to  $f(x, y) \rightarrow f(x + \frac{\pi}{\alpha}, y)$ . Consequently the bifurcation diagrams are symmetric with respect to the  $R$ -axis for any  $\alpha$ . Accordingly we draw only those parts of the diagram which lie above the  $R$ -axis. Two characteristics are observable. One is that the bifurcation branch stands steeper as  $\alpha$  decreases. The other is that, apart from a small neighborhood of the bifurcation point, the distance between the bifurcating branch and the basic flows seems to increase indefinitely as  $\alpha$  decreases to zero.

It is quite interesting that the branch is of different nature when  $\alpha$  is close to one. When  $0.966 \dots < \alpha < 1.0$ , the set of solutions of mode 1 is interestingly folded. When  $\alpha = 0.98$ , we have Fig.5 as a bifurcation diagram. In Fig.5, the primary bifurcation is supercritical. But we can observe two turning points on the branch. In Fig. 6 we present three figures of streamlines corresponding to the points A,B and C in Fig.5. The so called hysteresis observed in Fig. 5 disappears when  $\alpha$  becomes smaller than  $0.966 \dots$ . On the other hand, as we increase  $\alpha$ , the turning point on the right moves further to the right. When  $\alpha = 0.984$ , we have a pitchfork below and another branch with a turning point, which is substantially separated from the primary branch ( Fig. 8,9 ). Fig. 10 shows the case of  $\alpha = 0.999$ . In this case, the turning point in the upper side lies to the left of the pitchfork bifurcation point from the basic solution. This means existence of nontrivial solutions in the region  $R < R^*(\alpha)$ . This also implies that basic solution is stable but not globally stable if  $0 < 1 - \alpha$  is sufficiently small and  $R < R^*$  is sufficiently close to  $R^*$ .

In short, we can summarize as follows.

- 1) The bifurcating branch of mode one has no secondary bifurcation points, though there are turning points for  $\alpha < 1$  sufficiently close to 1.
- 2) At the primary bifurcation point, the bifurcation occurs supercritically, implying the stability of the new steady states in a neighborhood of the bifurcation point. This is in accord with the rigorously proven theorem that the primary bifurcation oc-

curs supercritically if  $\alpha$  is sufficiently small ([1,13,25]). Our numerical computation suggests that the theorem is true for all  $\alpha \in (0, 1)$ .

### §5. Solutions of mode two.

We next consider the solutions of mode two, which appear when  $0 < \alpha < 1/2$ . We first note that we have an obvious family of solutions of mode 2:  $(R, \alpha/2, \psi(2x, y))$  where  $\psi$  is a solution of mode one for  $\alpha$ . What is important is: there is a secondary bifurcation from this family. Thus, the structure of solutions of mode 2 is more complicated than that of the previous section. For later use, we prepare the following symbols:

M: main branch,      S: secondary branch,      1, 2, ...: mode.

For instance the solutions on the main branch of mode 2 is denoted by M2.

Let us see the solutions at  $\alpha = 0.35$ . Along the basic solutions there are two and only two bifurcation points. M1 solutions bifurcate at  $R^*(0.35) = 1.696438 \dots$ . M2 solutions bifurcate at  $R^*(0.7) = 3.011193 \dots$ . As we mentioned above, there is no secondary branch from the branch of mode one. On the other hand, there is a secondary branch which emanates from the branch of mode two. The secondary bifurcation occurs at  $R = R_s \equiv 4.807 \dots$ . It occurs supercritically. The streamlines of M2 and S2 flows are given in Fig. 12 and Fig. 13, respectively. The M2 solutions are unstable when  $R < R_s$ . They, however, recover the stability when  $R$  exceeds  $R_s$ . On the other hand, the S2 solutions are unstable for all  $R > R_s$ . Therefore the bifurcation diagram looks like Fig. 11, where the solid lines represent stable solutions and the broken lines do unstable ones. There is no turning point.

We next look at solutions when  $\alpha = 0.45$ . The bifurcation diagram is qualitatively the same as that of  $\alpha = 0.35$ . There is, however, a striking difference as for the stability. The M2 solutions are unstable for all  $R$  as well as S2 solutions. Therefore, the only stable solutions are M1 solutions ( see Fig. 11 ).

We now take a more precise look at the stability. We computed eigenvalues of the matrix which stem from the linearization at the M2 solutions. Suppose  $\alpha = 0.35$  and  $R$  is smaller than  $R_s$ . Then there is a real eigenvalue on the right half-plane, which implies the instability of the M2 solutions. All other eigenvalue are on the left half-plane. When  $R$  exceeds  $R_s$ , the unstable eigenvalue move to the left and crosses the imaginary axis at the origin, while all other eigenvalues are located in the left half-plane. Thus the M2 solution recovers stability at  $R_s$ . When  $\alpha = 0.45$ , there is one and only one unstable eigenvalue if  $R < R_s$ . When  $R$  exceeds  $R_s$ , the unstable eigenvalue remains in the right half-plane and an eigenvalue in the left half-plane crosses the imaginary axis at the origin. Thus the M2 solution remains to be unstable, having two real unstable eigenvalues for  $R > R_s$ .

The behaviour of the eigenvalues suggests that there is an  $\alpha_0 \in (0.35, 0.45)$  such that the linearized operator has zero eigenvalue with multiplicity two at  $R = R_s$ . Suggested by this, we computed bifurcation diagrams at  $\alpha = 0.43$ . No qualitative change is observed on M1 and S2 solutions. There is, however, a new phenomena

along the branch of M2 solutions. When  $R < R_s$ , then M2 solutions are unstable. At  $R = R_s$ , unstable S2 solutions bifurcates and the M2 solutions continues to be unstable, having two real unstable eigenvalues. The similarity between the case of  $\alpha = 0.43$  and that of 0.45 ends when  $R$  exceeds a certain value  $R_h \approx 13.85$ . There a Hopf bifurcation occurs at M2 branch. When  $R > R_h$ , the M2 solutions recover stability ( Fig. 14 ). Before Hopf bifurcation occurs, the two real unstable eigenvalues coalesces to a pair of complex conjugate eigenvalues. At  $R = R_h$ , this pair crosses the imaginary axis from the right half plane to the left half. We can not say anything about the stability of the periodic solution yielded by the Hopf bifurcation. Table 1 shows qualitative behaviour of the eigenvalues.

An even more interesting bifurcation of stationary solutions is present when  $\alpha$  is sufficiently close to 0.5. Fig.15, 16 and 17 show the case of  $\alpha = 0.49, 0.4905$  and  $0.4876$ , respectively.

### §7. Solutions of mode three.

For  $0 < \alpha < 1/3$ , there are solutions of mode three.

At  $\alpha = 0.3$  we have three bifurcation points on the branch of the basic flows. These are  $R^*(0.3), R^*(0.6), R^*(0.9)$ . These correspond to the bifurcation of mode one, two, three, respectively. Solutions of mode one and two are qualitatively the same as those at  $\alpha = 0.35$ . Along M3 branch, we computed the eigenvalues. As  $R$  increases from  $R^*(0.9)$ , the number of unstable solutions varies as 2, 3, 2, 4. When the number changes from 2 to 4, a Hopf bifurcation occurs. In order to further study the solutions of mode three, more freedom of degree seems to be needed and our results here are indecisive. This laborious work will be done in the future.

### REFERENCES

1. A.L. Afendikov and K.I. Babenko, *Bifurcation in the presence of a symmetry group and loss of stability of some plane flows of a viscous fluid*, Soviet Math. Dokl. **33** (1986), 742-747.
2. K.I. Babenko and M.M. Vasil'ev, *Stability of incompressible fluid flows on a plane torus*, Soviet Phys. Dokl. **32** (1987), 541-543.
3. S.O. Belotserkovskii, A.P. Mirabel' and M.A. Chusov On the construction of the post-critical mode for a plane periodic flow, *Izv. Atmos. Oceanic Phys.* **14** (1978), 6-12.
4. N.F. Bondarenko, M.Z. Gak and F.V. Dolzhanskii, *Laboratory and theoretical models of plane periodic flows*, *Izv. Atmos. and Oceanic Phys.* **15** (1979), 711-716.
5. V. Franceschini, C. Tebaldi and F. Zironi, *Fixed point limit behavior of N-mode truncated Navier-Stokes equations as N increases*, *J. Statis. Phys.* **35** (1984), 387-397.
6. K. Gotoh and M. Yamada, *Instability of a cellular flow*, *J. Phys. Soc. Japan* **53** (1984), 3395-3398.
7. K. Gotoh and M. Yamada, *The instability of rhombic cell flows*, *Fluid Dyn. Res.* **1** (1986), 165-176.
8. K. Gotoh, M. Yamada and J. Mizushima, *The theory of stability of spatially periodic parallel flows*, *J. Fluid. Mech.* **127** (1983), 45-58.
9. R. Grappin, J. Leorat and P. Londrillo, *Onset and development of turbulence in two dimensional periodic shear flows*, *J. Fluid. Mech.* **195** (1988), 239-256.
10. J.S.A. Green, *Two-dimensional turbulence near the viscous limit*, *J. Fluid. Mech.* **62** (1974), 273-287.

11. V.I. Iudovich, *Example of the generation of a secondary stationary or periodic flow when there is loss of stability of the laminar flow of a viscous incompressible fluid*, J. Appl. Math. Mech. **29** (1965), 527–544.
12. T. Kambe and Y. Kamanaka, *Nonlinear dynamics of two-dimensional flows: bifurcation, chaos and turbulence*, to appear in Proc. Nonlinear Dynamics of Structures ( Moscow-Permi Symposium ), World Scientific.
13. M. Katsurada, H. Okamoto and M. Shōji, *Bifurcation of the stationary Navier-Stokes flows on a 2-D torus*, to appear in " Proc. Katata Workshop on Nonlinear PDEs and Applications ", eds. M. Mimura and T. Nishida.
14. H.B. Keller, "Lectures on Numerical Methods in Bifurcation Theory ( Tata Institute of Fundamental Research No. 79 )," Springer verlag, 1987.
15. S. Kida, M. Yamada and K. Ohkitani, *The energy spectrum in the universal range of two dimensional turbulence*, Fluid Dynam. Res. **4** (1988), 271–301.
16. S. Kida, K. Ohkitani and M. Yamada, *Triply periodic motion in a Navier-Stokes flow*, J. Phys. Soc. Japan **58** (1989), 2380–2385.
17. C. Marchioro, *An example of absence of turbulence for any Reynolds number*, Commun. Math. Phys. **105** (1986), 99–106.
18. L.D. Meshalkin and Y.G. Sinai, *Investigation of the stability of a stationary solution of a system of equations for the plane movement of an incompressible viscous liquid*, J. Appl. Math. Mech. **25** (1962), 1700–1705.
19. B. Nicolaenko and Z.-S. She, *Coherent structures, homoclinic cycles and vorticity explosions in Navier-Stokes flows*, in " Topological Fluid Mechanics ", eds. H.K. Moffatt and A. Tsinober (1990), 265–277.
20. A.M. Obukhov, *Kolmogorov flow and laboratory simulation of it*, Russian Math. Surveys **38:4** (1983), 113–126.
21. A.M. Obukhov, F.V. Dolzhanskii and A.M. Batchaev *A simple hydrodynamic system with oscillating topology*, in " Topological Fluid Mechanics ", eds. H.K. Moffatt and A. Tsinober (1990), 304–314.
22. G.I. Sivashinsky, *Weak turbulence in periodic flows*, Physica **17D** (1985), 243–255.
23. M. Takaoka, *Stability of triangular cell flows*, J. Phys. Soc. Japan **58** (1989), 2223–2226.
24. C. Tebaldi, *Fixed points behaviour in truncated two-dimensional Navier-Stokes equations*, in " Nonlinear Dynamics ", ed. G. Turchetti, World Scientific (1989), 412–422.
25. M. Yamada, *Nonlinear stability theory of spatially periodic parallel flows*, J. Phys. Soc. Japan **55** (1986), 3073–3079.

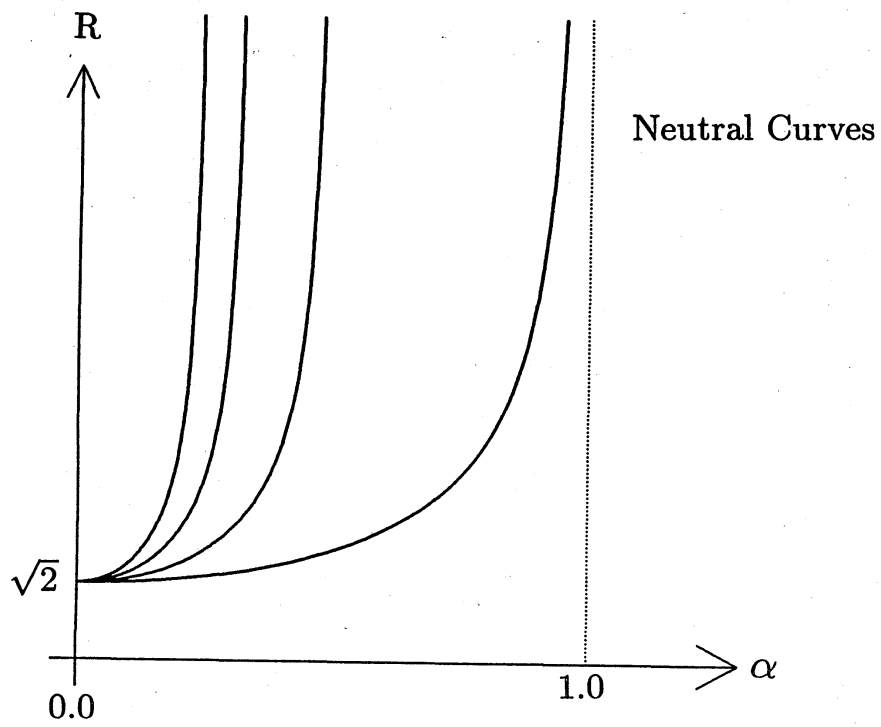


Fig. 1 : Neutral curves ( = bifurcation curves ) with mode 1,2,3 and 4.

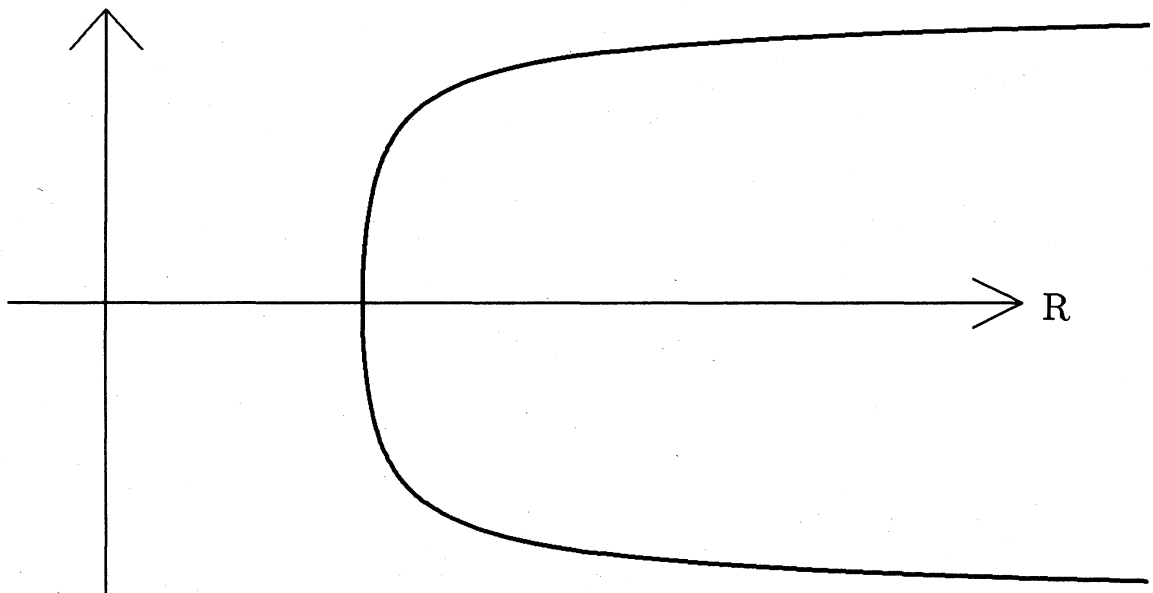


Fig. 2 : Schematic bifurcation diagram when  $\alpha = 0.7$ .

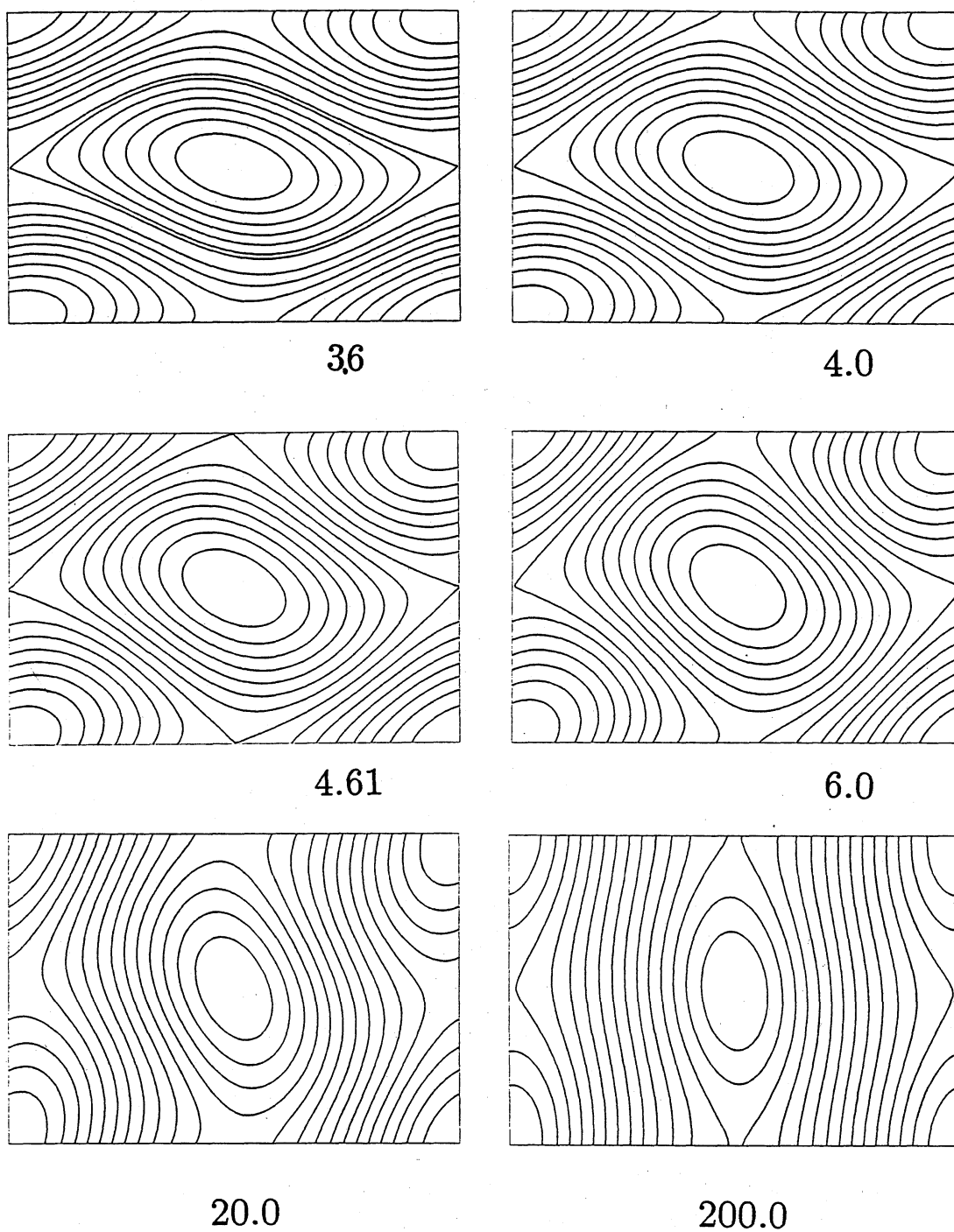


Fig. 3 : Stream lines when  $\alpha = 0.7$ . The Reynolds numbers are 3.6, 4.0, 4.61, 6.0, 20.0 and 200.0, respectively.

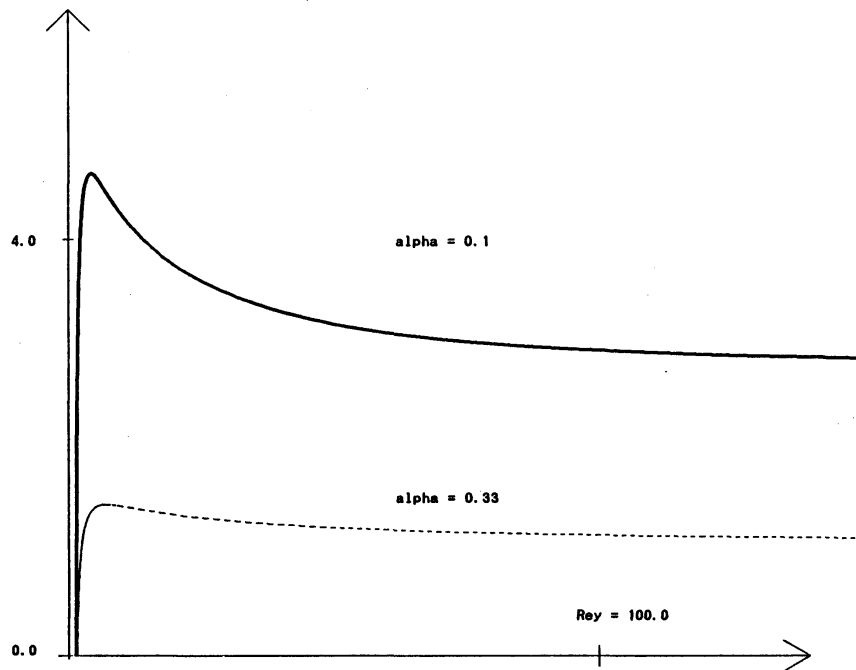


Fig. 4 : Bifurcation diagrams with  $\alpha = 0.33$  and  $0.1$ . Only upper halves are drawn. Here and in the following figures, the ordinate represents  $|a(0,1) - 1/2| + |a(1,0)|$ .

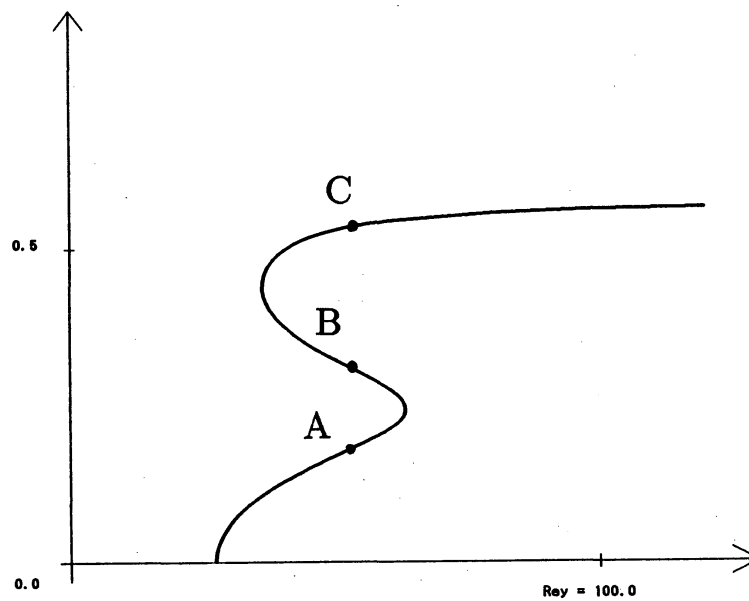


Fig. 5 : Bifurcation diagram when  $\alpha = 0.98$ .

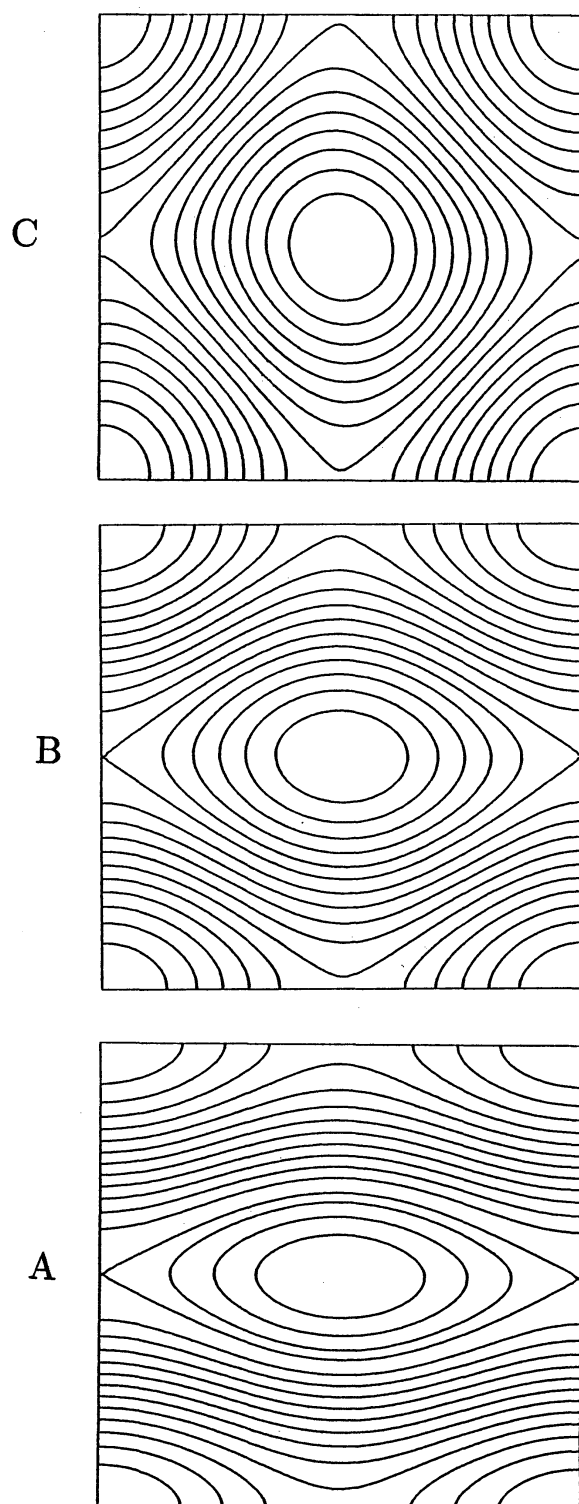


Fig. 6 : Stream lines of solutions corresponding to points A, B and C in Fig. 5.



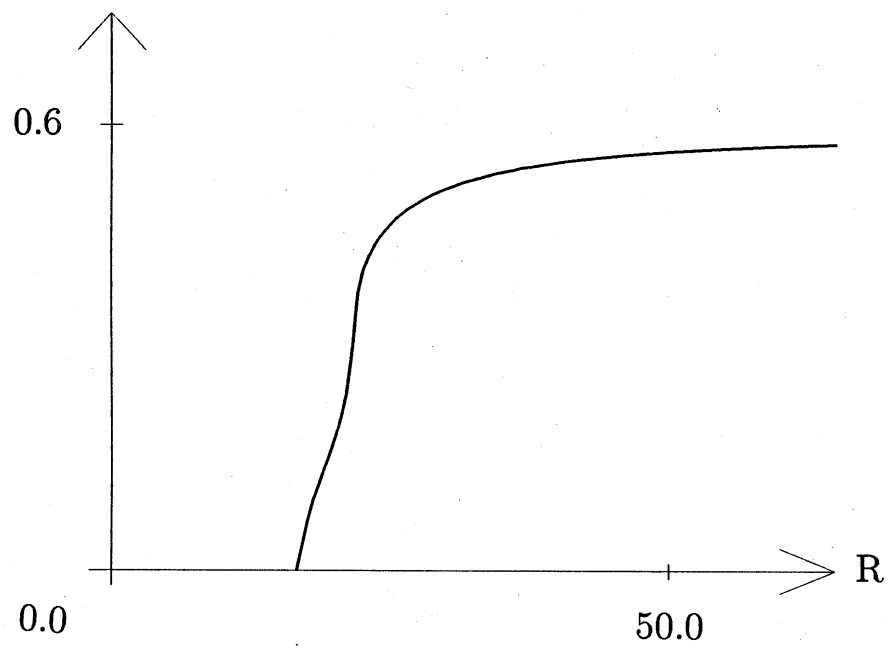


Fig. 7 : Bifurcation diagram when  $\alpha = 0.966$ .

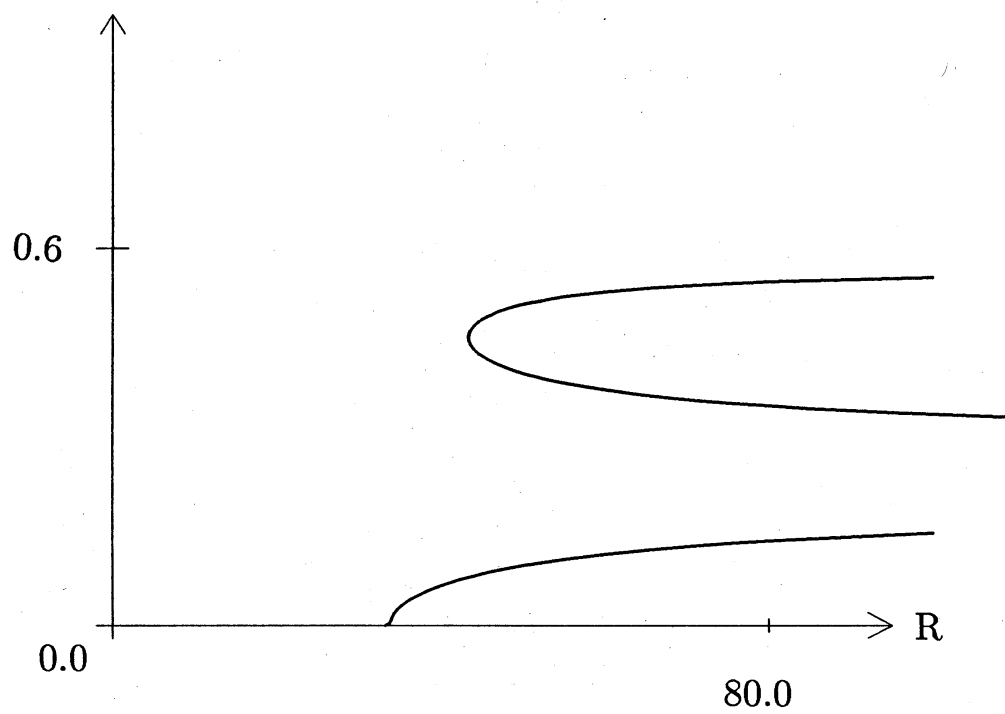


Fig. 8 : Bifurcation diagrams when  $\alpha = 0.984$

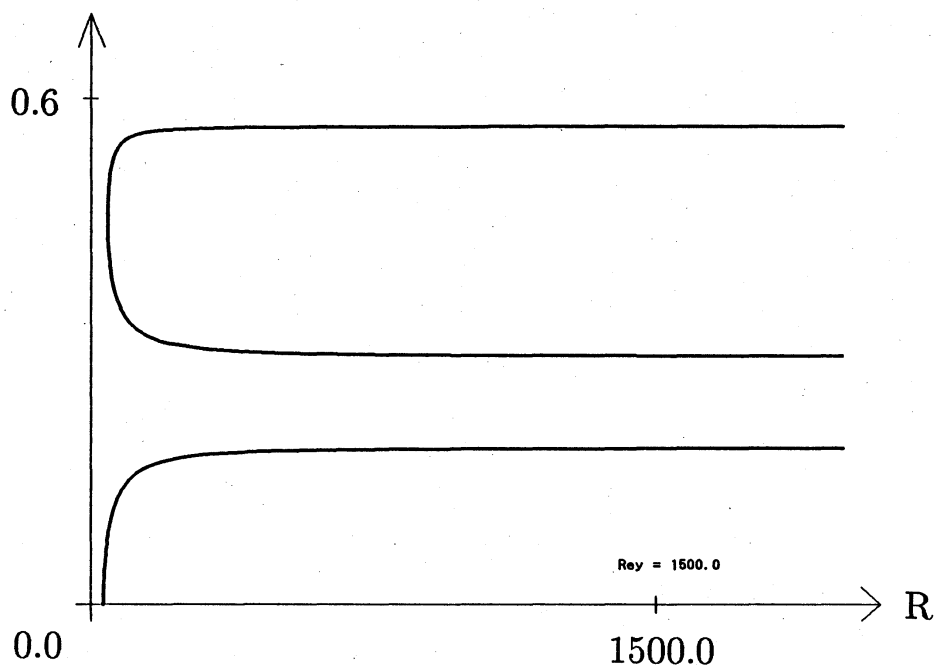


Fig. 9 : Bifurcation diagrams when  $\alpha = 0.984$  with different scales.

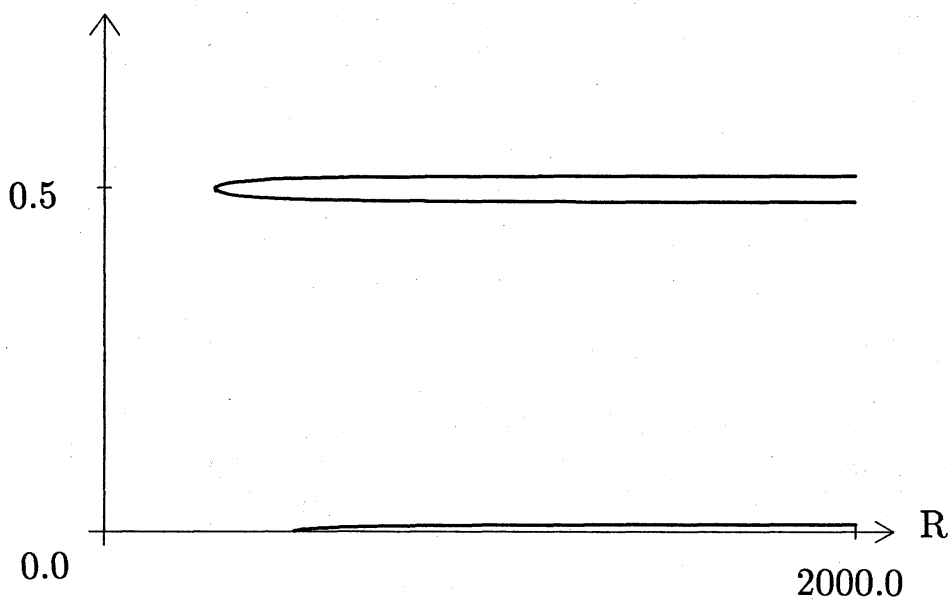


Fig. 10 : Bifurcation diagram when  $\alpha = 0.999$ .

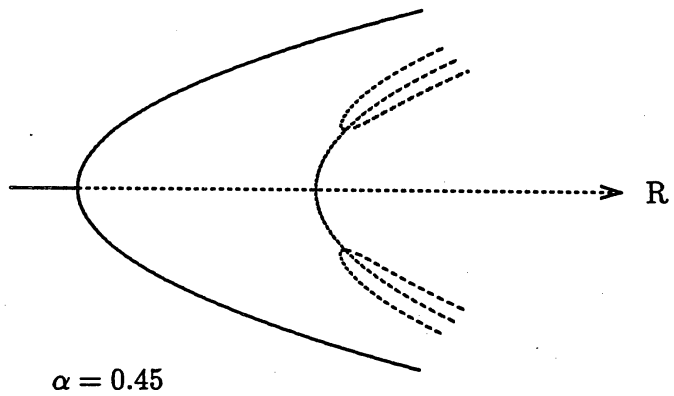
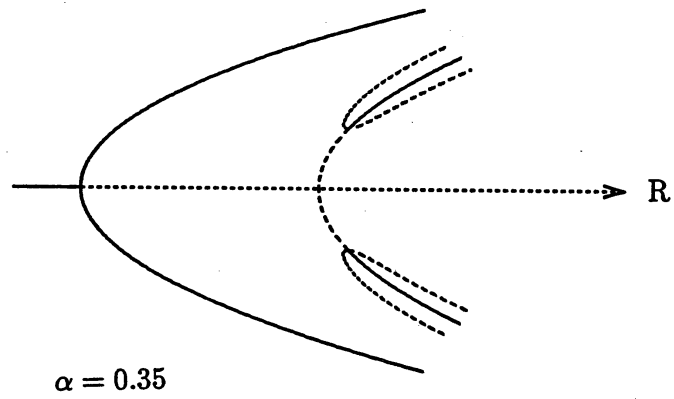


Fig. 11 : Schematic bifurcation diagrams when  $\alpha = 0.35$  and  $0.45$ . Solid lines indicate that the solution is stable. Broken lines indicate that they are unstable.

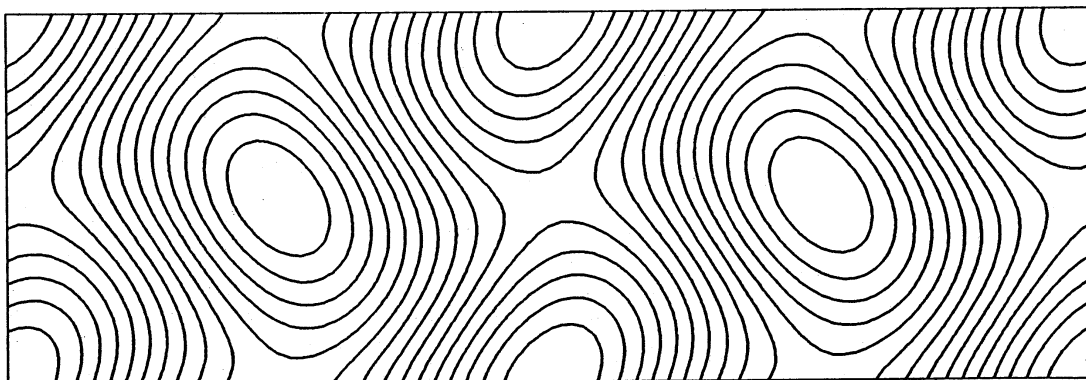
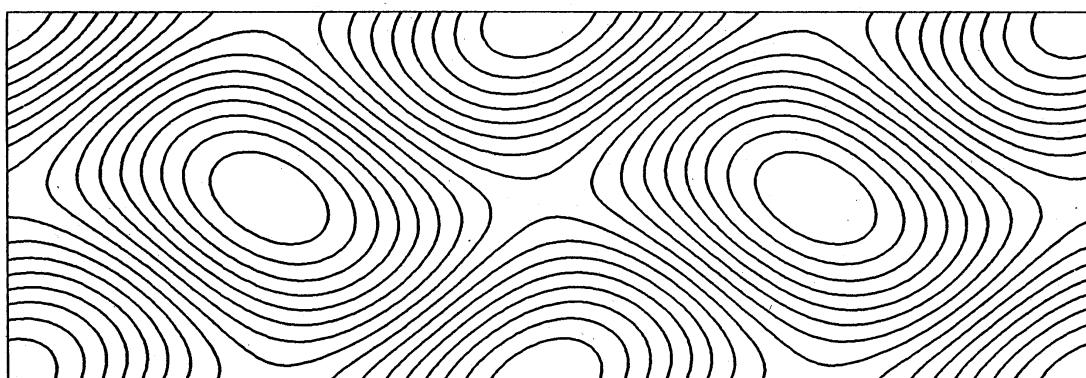
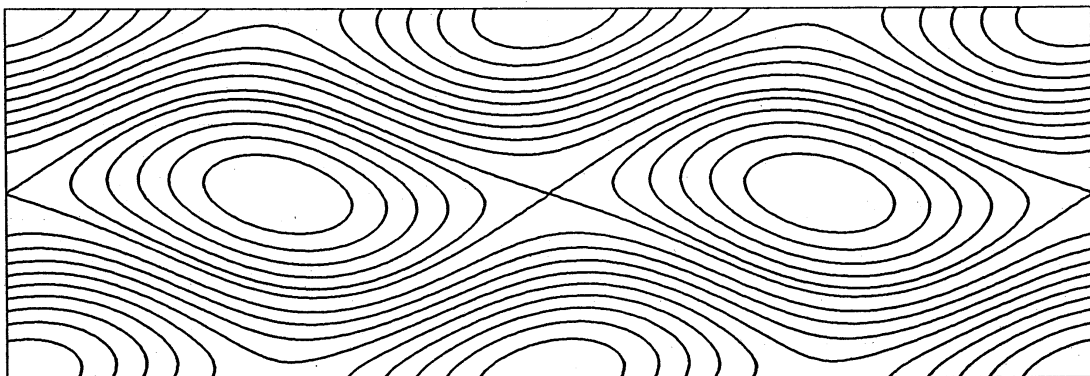


Fig. 12 : Stream lines of M2 solutions.  $\alpha = 0.35$ .

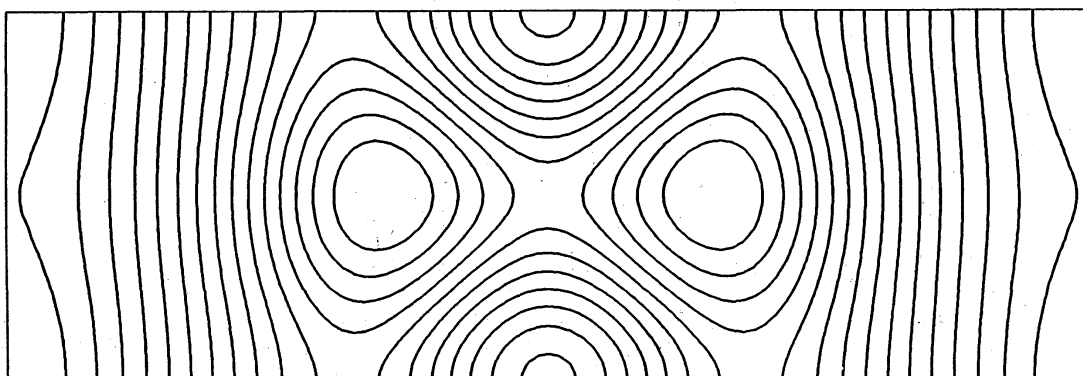
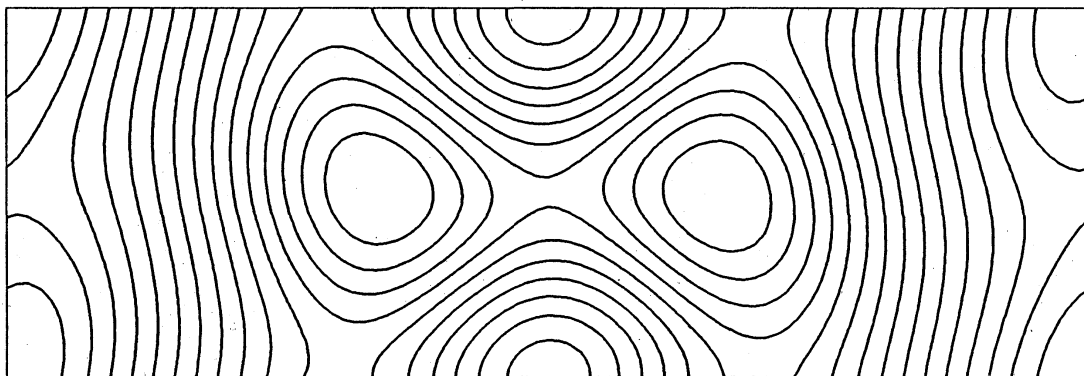
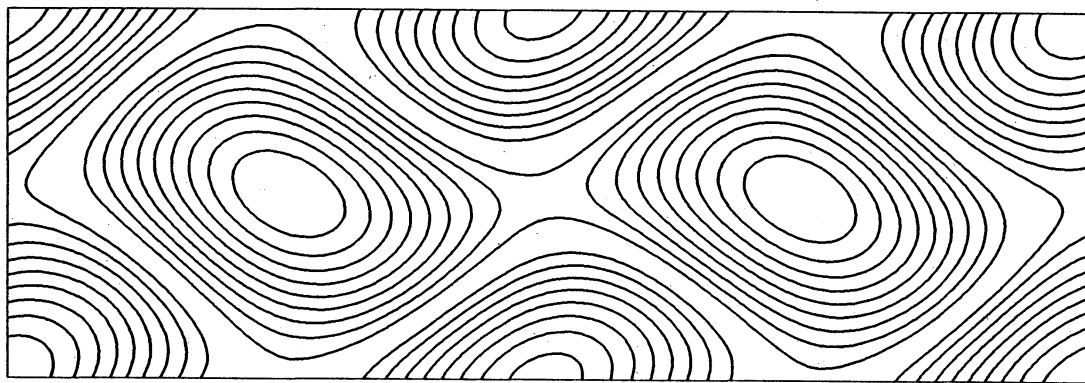


Fig. 13 : Stream lines of S2 solutions.  $\alpha = 0.35$ .

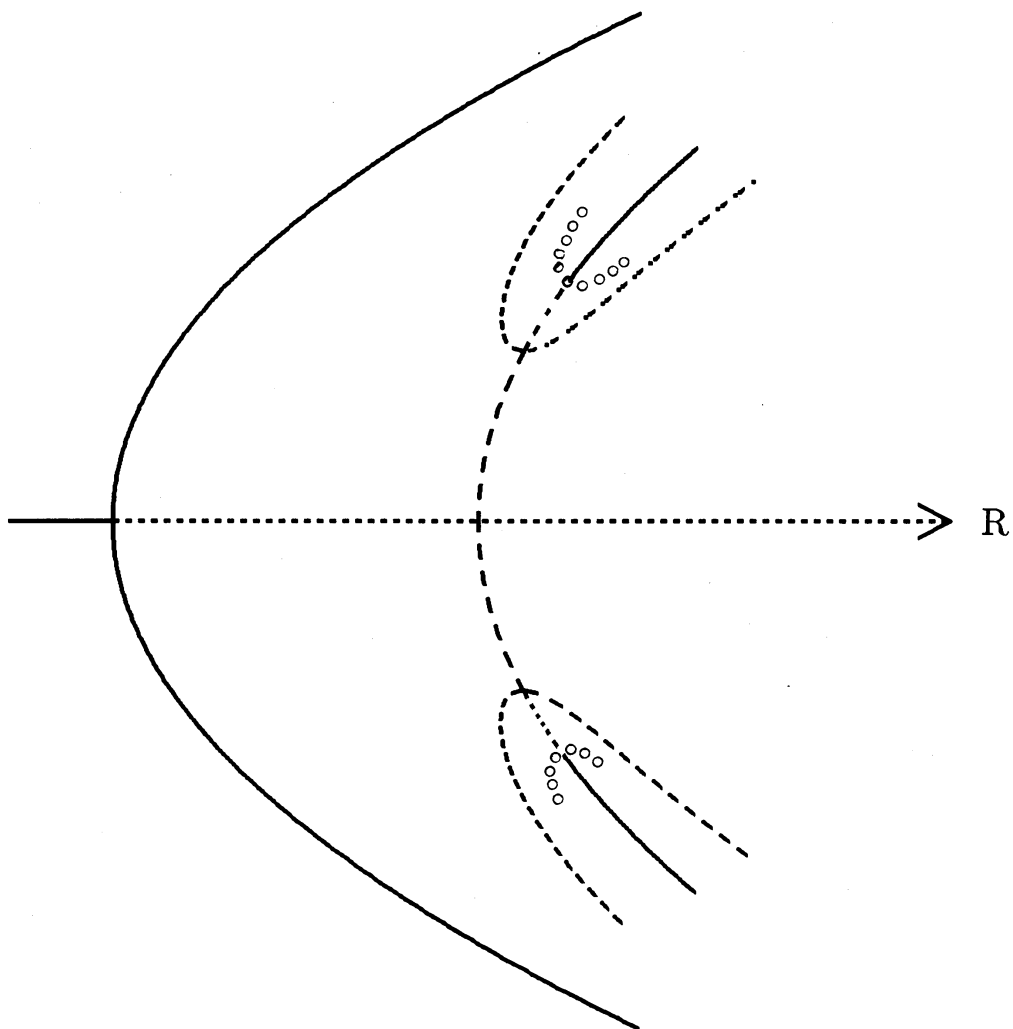


Fig. 14 : Bifurcation diagram when  $\alpha = 0.43$ . The direction of the Hopf branch is uncertain.

Hopf branch : ○○○○○○

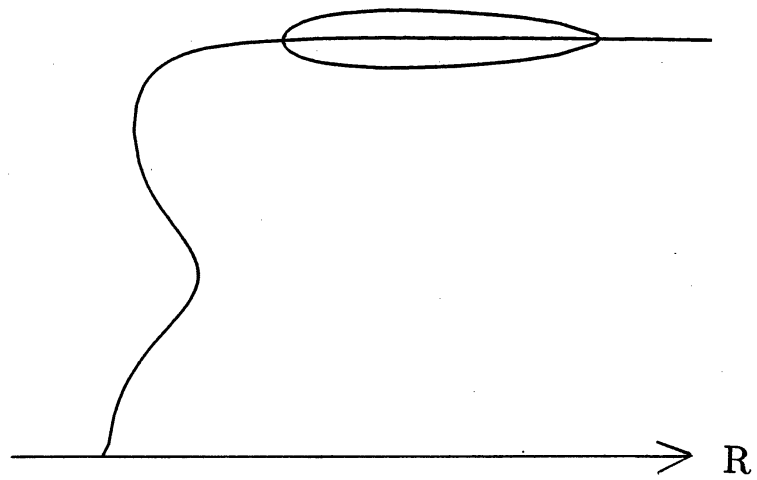


Fig. 15 : Bifurcation diagram when  $\alpha = 0.49$ .

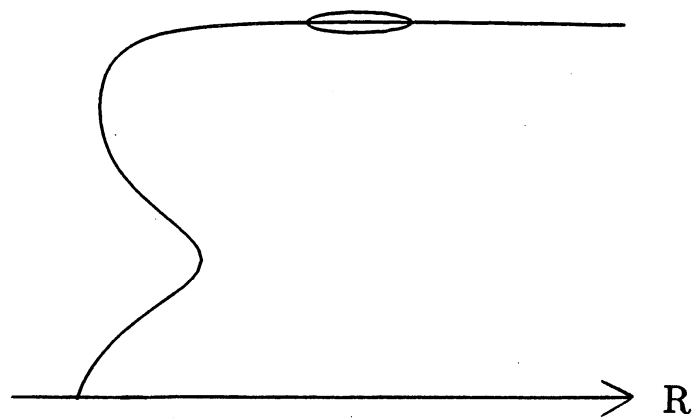


Fig. 16 : Bifurcation diagram when  $\alpha = 0.4905$ .

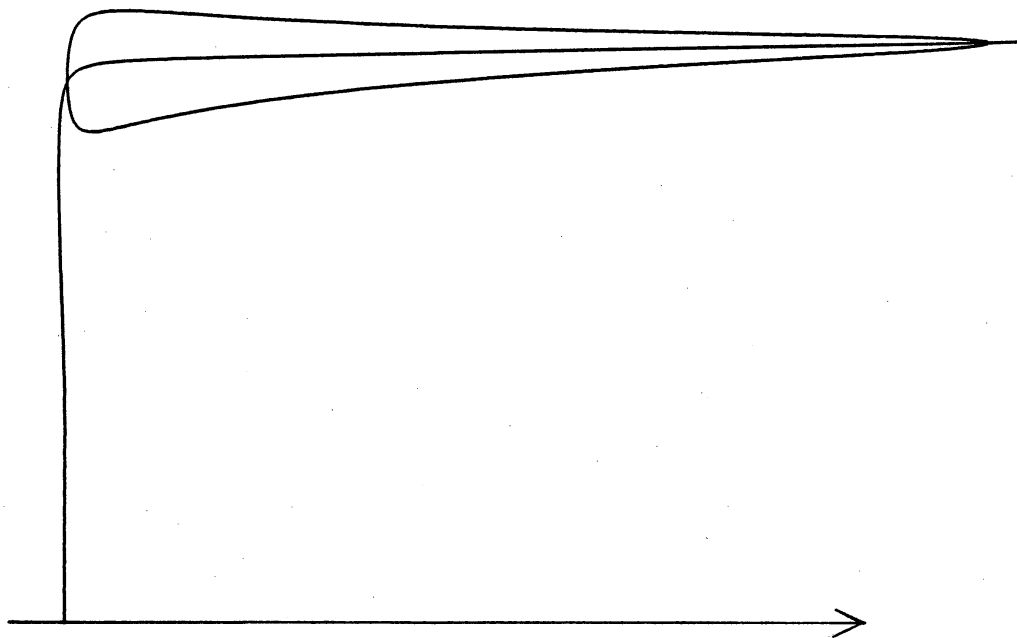


Fig. 17 : Bifurcation diagram when  $\alpha = 0.4876$ .